Boosting Financial Risk Prediction Model Using Attention Mechanism Based Recurrent Neural Networks with Red-Tailed Hawks Algorithm

Ilyos Abdullayev[1,*], Hafis Hajiyev[2], Mahfuza Sattarova[3], Elena Klochko[4]

[1]Department of Business and Management, Urgench State University, Urgench, 220100, Uzbekistan

[2]Department of Finance and Audit, Azerbaijan State University of Economics (UNEC), Baku, AZ1001, Republic of Azerbaijan

[3]Department of Economics, Mamun University, Khiva, 220900, Uzbekistan

[4]Department of Management, Kuban State Agrarian University named after I.T. Trubilin, Krasnodar, 350044, Russia

Emails: ilyos.a@urdu.uz; hafiz_hajiyev@unec.edu.az; sattarova_maxfuza@mamunedu.uz; klochko.e.n@yandex.ru

Abstract

The systemic prediction of financial risk issues has become a main attention in the area of finance. Financial risk is the main likelihood that stockholders will lose currency after they finance a business that has debt if the business flow of cash demonstrates insufficient to see its economic requirements. The incorporation of deep learning (DL) methods into financial risk forecast and investigation has altered conventional techniques. While traditional quantitative systems often trust basic metrics such as the highest reduction, the arrival of DL requires a more nuanced assessment, highlighting the model's generalization capability, particularly in market crises like stock market crashes. DL techniques are efficient in removing intricate patterns from massive data collections and become an effective model for forecasting financial trends. In this paper, we offer Boosting Financial Risk Prediction Model Using Attention Mechanism with Red-Tailed Hawk (BFRPM-AMRTH) Algorithm. The presented BFRPM-AMRTH model aims to address the challenges of identifying and mitigating potential financial threats in a dynamic environment. Initially, the BFRPM-AMRTH technique applies the linear scaling normalization (LSN) data normalization technique to standardize the input features and ensure consistency across the dataset. In addition, the long short-term memory auto encoder with attention mechanism (LSTMA-AE) technique can be employed for classifying financial risks. Eventually, the red-tailed hawk (RTH) algorithm adjusts the hyperparameter values of the LSTMA-AE algorithm optimally and outcomes in greater classification performance. To ensure the improved performance of BFRPM-AMRTH system, a huge range of simulation studies has been achieved and the obtained outcomes establish the advancement of the BFRPM-AMRTH system over the existing techniques

Keywords: Financial Risk Prediction; Red-Tailed Hawk Algorithm; Attention Mechanism Linear Scaling Normalization; Deep Learning

1. Introduction

Financial risk is the chance that stockholders will lose funds while they capitalize on the business that has debt when the company's flow of cash shows insufficient to see its economic debts [1]. While a corporation utilizes debt financing, its customers are recompensed earlier than its stockholders are when the corporation becomes ruined. Financial risk is frequently sensed as the risk that a corporation might default on its debt payments [2]. To extract possible financial risks and be capable of recognizing the intensity of corporate economic health, forecast methods are utilized, sensed as a proper warning approach to approaching concerns in the inspected corporations [3]. Their job is to assess the economic strength of the business depending on designated economic indicators or other features of the corporation or the setting in which they work [4]. Economic security is the essential for

DOI: https://doi.org/10.54216/FPA.180202
Received: July 29, 2024 Revised: October 30, 2024 Accepted: January 03, 2025

national financial security, so we need to attach better significance to possible hazards in the economic domain and determinedly keep the avoiding bottom-line hazards. To preclude the economic hazards with the lowest cost, precise economic hazards forecast technique is required [5].

Financial crisis prediction (FCP) is embedded in the detection of the substantial social and economic effects that economic crises can have on a worldwide level [6]. Economic crises may cause unemployment, massive economic losses, and losses in asset principles, resulting in significantly affecting individuals and businesses [7]. FCP aids economic organizations in making decisions at the appropriate period for balanced development. Generally, FCP produces a binary classification model, which is sensibly determined. Improper decision-making in a company may cause bankruptcy or financial failure and clients, vendors, investors, and more. The ongoing process in information technology domain to achieve each type of data is densely connected to the initiative's risk levels [8]. A wide range of individuals depends on the analyst's decision to assess a huge variety of data. Nowadays dynamic economic landscape, the incorporation of Deep Learning (DL) methodologies has modernized the method of risk analysis and prediction. Conventional quantitative models frequently depend on metrics such as maximum drawdown to assess risk control capability [9]. Nevertheless, with the initiation of DL, there is developing hazard valuation that wants a more nuanced knowledge, encompassing beyond simplistic actions. DL methods present unparalleled sophistication in taking dynamics and complicated patterns in economic data [10]. However, their effectiveness in managing hazards hinges not merely on statistical metrics but also on their generalizability and their capability to modify to unexpected market settings, particularly in crises like stock market crashes.

This paper offers Boosting Financial Risk Prediction Model Using Attention Mechanism with Red-Tailed Hawk (BFRPM-AMRTH) Algorithm. Initially, the BFRPM-AMRTH technique applies the linear scaling normalization (LSN) data normalization technique to standardize the input features and ensure consistency across the dataset. In addition, the LSTMA-AE technique can be employed for classifying financial risks. Eventually, the red-tailed hawk (RTH) algorithm adjusts the hyperparameter values of the LSTMA-AE algorithm optimally and outcomes in greater classification performance. To ensure the improved performance of BFRPM-AMRTH system, a huge range of simulation studies has been achieved.

2. Literature Survey

In [11], a DNN-based aiding decision method for economic risk forecast in the carbon trading market is projected for this target. Subsequently, the DNN is employed for quantitative investigation and to create an intellectual decision structure that outputs economic risk forecast outcomes. Venkateswarlu et al. [12] introduce an oppositional ant lion optimizer-based feature selection with ML-enabled classification (OALOFS-MLC) method for FCP in big data settings. Additionally, the developed OALOFS-MLC approach intends an innovative OALOFS model to select finest feature subsets that assist in attaining enhanced classification outcomes. Wu et al. [13] projected a stock market prediction method associating an MLP-ANN with the conventional Altman Z-Score technique. The involvement of this study is demonstration of a novel hybrid business crisis cautionary technique associating MLP-ANN and Z-score methodologies.

Ju and Zhu [14] deliberate the RL application in economic strength risk evaluation, particularly how to enhance the capability of risk forecast and investment portfolio optimizer over DRL techniques. Conventional economic risk evaluation approaches are frequently incapable of effectually coping with the dynamic variations and economic market difficulties, nevertheless, RL technology offers novel solutions for latest economic risk management by using real-world adaptation and adjustment modules. Li et al. [15] primarily propose the enhanced BP neural method as the economic initial cautionary method and safeguard its higher forecast precision. During this investigation, the process source and connected reasoning procedure of this method are defined, its limitations are examined, and solutions are put forward.

Yang et al. [16] discover the decisive features of assessing DL technique's hazard control ability in finance, emphasizing the significance of recognizing either statistical measures or generalizability, mainly in opposing market settings. By analyzing DL technique's performance in situations such as stock market crashes and emphasizing the importance of cross-validation models, this paper focused on providing practitioners with visions for structuring strong risk organization methods. It supports an inclusive method incorporating quantitative analysis with macroeconomic features to improve economic risk forecast and analysis in explosive markets. In [17], this study organizes experiential research with an example of listed Chinese e-commerce initiatives from 2012-22. Primarily, utilizing FA to attain the general features among the unique non- and financial indexes has the impact of decreasing the overfitting method risk. Then, the output of MSE and the LSTM neural network predicted values are utilized. Eventually, an economic risk forecast technique dependent on FA-PSO-LSTM DL is developed, and many benchmarking models are recommended to the comparative survey on any evaluation index.

3. The Proposed Methodology

DOI: https://doi.org/10.54216/FPA.180202
Received: July 29, 2024 Revised: October 30, 2024 Accepted: January 03, 2025

In this paper, we offer BFRPM-AMRTH Algorithm. The presented BFRPM-AMRTH model aims to address the challenges of identifying and mitigating potential financial threats in a dynamic environment. Fig. 1 represents the complete workflow of BFRPM-AMRTH model.

A. Data Normalization

Primarily, the BFRPM-AMRTH model applies the LSN data normalization technique to standardize the input features and ensure consistency across the dataset. LSN is a data pre-processing model, which regulates financial datasets by converting features within the range of [0, 1], or [-1, 1]. In Financial Risk forecast, LSN certifies that every input variable is on a similar measure, which aids in enhancing model accuracy and convergence. By removing differences in data magnitude, LSN improves the performance of ML methods, particularly those delicate to feature scale. This normalization method is chiefly beneficial in financial data, where dissimilar metrics, like stock prices or loan amounts, differ generally. LSN donates to a more stable representation of data, certifying trustworthy and effectual prediction of financial risk.

B. Classification using LSTMA-AE

In addition, the LSTMA-AE technique can be employed for classifying financial risks. LSTM is the different kind of Recurrent Neural Network (RNN) structure [18]. The basic invention of LSTM rests in its presentation of 3 gate elements: the input, output, and forget gates. These gating elements permit LSTM to adaptively select which data must be preserved in the cell of the memory, thus enhancing its implementation in modeling longer sequences.

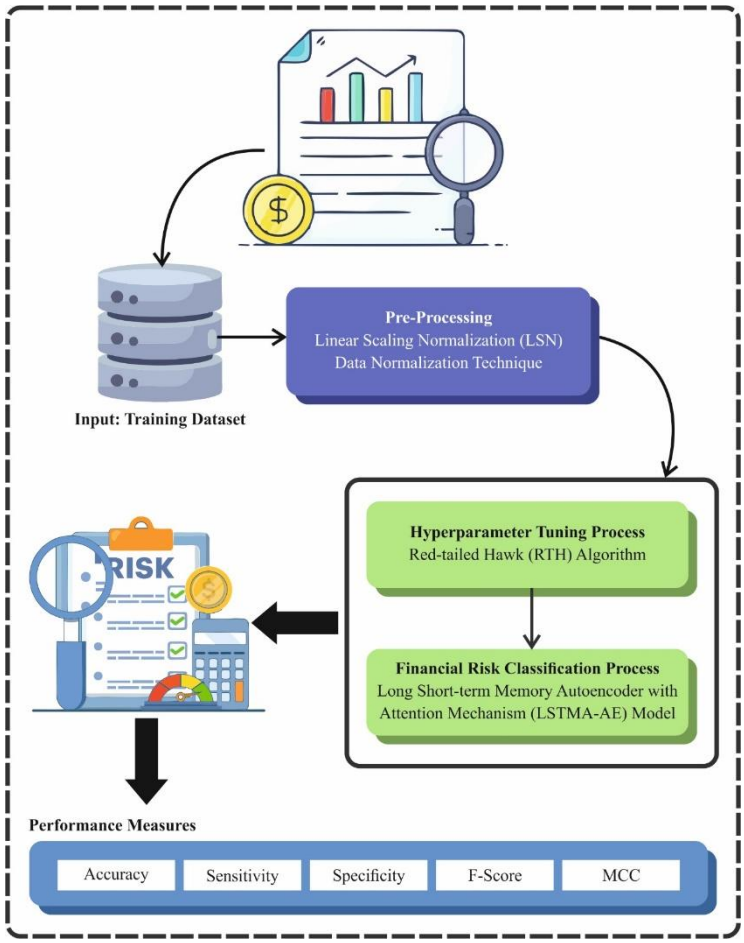

Figure 1. Overall flow of BFRPM-AMRTH Algorithm

This method is the DL method, which incorporates AE and LSTM technologies, mainly appropriate for analyzing and processing time-series data. This method contains dual major modules: the Decoder and the Encoder. Encoding seizures the time-based dependences and characteristics of the sequence of input over numerous layers of LSTM, whereas the Decoding has the responsibility for rebuilding the novel time-series data from the concealed representations produced by the Encoding, maintaining the key characteristics and data of the input information. Here, X_t characterizes the input, H_t signifies the hidden layer (HL), F_t represents forget gate, I_t denotes input gate,

DOI: https://doi.org/10.54216/FPA.180202
Received: July 29, 2024 Revised: October 30, 2024 Accepted: January 03, 2025

O_t symbolize output gate, C_t refers to candidate memory cell, C_t stands for memory cell at the present times t. The particular computation is presented as Eq. (1),

$$\begin{aligned} F_t &= \sigma(W_f \cdot [H_{t-1}, X_t] + b_f) \\ I_t &= \sigma(W_i \cdot [H_{t-1}, X_t] + b_i) \\ \tilde{C}_t &= \tanh(Wc \cdot [H_{t-1}, X_t] + b_C) \\ C_t &= F_t^* C_{t-1} + I_t^* \tilde{C}_t \\ o_t &= \sigma(W_o \cdot [H_{t-1}, X_t] + b_o) \\ H_t &= O_t^* \tanh(C_t) \end{aligned} \tag{1}$$

Whereas σ and $tanh$ characterize the activation function of the Sigmoid and hyperbolic tangent. W_i, W_f, W_o and W_c characterize the weighted matrices for the forget, input, output gates, and cell state of the candidate memory, correspondingly b_i, b_f, b_o and b_c represent the biased terms for the forget, input, output gates, and cell state of the candidate memory, correspondingly $\odot$ embodying the element-to-element multiplication operator.

Owing to the diversity and complexity of the multiple-variable time-series data produced in the process of vaccination forces, while all dimensions might imitate dissimilar physical amounts like temperature, pressure, and rate of flow, conventional LSTM-AE techniques might fight with taking composite temporal interactions and dependencies. They might additionally have trouble underlining significant information through dissimilar time steps or particular unread data. Hence, they have presented an AM into the LSTM-AE algorithm. This study combines temporal design AM into the computation of the HL within the LSTM-AE method to improve the capability of the models for learning from data at dissimilar time steps. The AM assistances the method dynamically fine-tuning the influence of all input information of the time steps to the HL, improving seizing significant data while ignoring unrelated details, thus enhancing the algorithm's modeling ability. For every decoding time step t, they compute the scores of attention amongst each of the HL of the encoding $h_i (i = 1,2, \dots, t)$ and the present HL h'_t of the decoder Eq. (2).

$$e_{ti} = score\ (h'_t, h_i) \tag{2}$$

Now, we utilize the additional AM, with its computation provided by Eq. (3).

$$e_{ti} = v^T \tanh(W_1 h'_t + W_2 h_i) \tag{3}$$

In that regard, v^T, W_1, W_2 are learning parameter matrices. The scores of attention are then standardized to get the attentional weighting for all HL Eq. (4).

$$\alpha_{ti} = \frac{\exp(e_{ti})}{\sum_{j=1}^{t} \exp\ (e_{tj})} \tag{4}$$

Following, the context vector of the weighted average is computed as Eq. (5).

$$c_t = \sum_{i=1}^{t} \alpha_{ti}\, h_i \tag{5}$$

The vector of the context C_t comprises the weighting data of each of the HLs of the encoder, which well signifies the significant attributes data of the sequence of input at present step. The vector of the context C_t is formerly presented in the decoding. The LSTM component of the decoding is computed as Eq. (6),

$$h'_t = LSTM([y_{t-1}, c_t], h'_{t-1}) \tag{6}$$

Whereas y_{t-1} characterizes the preceding step's decoding output, c_t characterizes the present context vector time steps, and h'_{t-1} characterizes the preceding HL steps. The present HL h'_t is then mapped to the output area over linear transformations to get the present output time step's y_t Eq. (7).

$$y_t = Linear(h'_t) \tag{7}$$

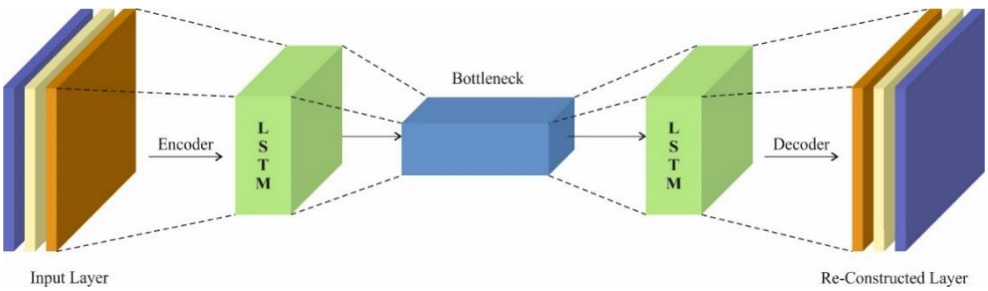

DOI: https://doi.org/10.54216/FPA.180202
Received: July 29, 2024 Revised: October 30, 2024 Accepted: January 03, 2025

Figure 2. Architecture of LSTMA-AE technique

Accordingly, once the decoder makes a novel HL h_t at all steps, it completely uses the global information from the HL of the encoders, thus enhancing the performance of the model. It can well seize and balance information through dissimilar time steps, successfully capturing composite interaction effects and temporal dependences. The model carries out well on training data and shows stronger generalizability on hidden data, making it stronger in real-world applications. Fig. 2 depicts the infrastructure of the LSTMA-AE technique.

C. Hyperparameter Tuning Process

Eventually, the RTH algorithm adjusts the hyperparameter values of the LSTMA-AE algorithm optimally and outcomes in greater classification performance. The RTH model is stimulated by the RTH searching behavior [19]. At the time of hunting, the RTH goes over three stages such as low soaring, high soaring, and swooping. The mathematic representation of these 3 stages is given below:

High-Soaring Phase

In an RTH's hunting, it climbs over the sky to discover food in a better way. This behavior is mathematically formulated in Eq. (8).

$$X(t) = X_{best} + \left(X_{mean} - X(t-1)\right) * Levy(dim) * TP(t) \tag{8}$$

Here, $X(t)$ means the current location of RTH, X_{best} refers to the present optimum location, X_{mean} is the current average location, $Levy(dim)$ means the function of Levy fight distribution, which is defined utilizing Eq. (9), and $TF(t)$ signifies the function of transition factor, which is computed utilizing Eq. (11).

$$Levy(dim) = s * \frac{\mu * \sigma}{|v|^{\beta-1}} \tag{9}$$

Here, s and β are a constant with a value of 0.01 and 1.5, correspondingly. dim refers to dimension of problem, and μ and v are arbitrarily generated numbers within the interval of [0 1]. σ is computed as per Eq. (10).

$$\sigma = \left(\frac{\Gamma(1+\beta) * \sin\left(\frac{\pi\beta}{2}\right)}{\Gamma\left(1+\frac{\beta}{2}\right) * \beta * 2^{\left(1-\frac{\beta}{2}\right)}} \right) \tag{10}$$

$$TF(t) = 1 + \sin\left(2.5 + \left(\frac{t}{T_{\max}}\right)\right) \tag{11}$$

While, $T_{\max}$ is the maximum iteration count.

Low-Soaring Phase

Once appropriate prey is over the high-soaring stage, the RTH will glide lower to latch onto the prey for improved pursuit. This behavior can be demonstrated as presented in Eq. (12).

$$X(t) = X_{best} + \left(x(t) + y(t)\right) * StepSize(t) \tag{12}$$

Whereas $StepSize(t)$ is measured depending on Eq. (13).

$$StepSize(t) = X(t) - X_{mean} \tag{13}$$

Here x and y signify directional coordinates, calculated utilizing Eq. (14).

$$\begin{cases} x(t) = R(t) * \sin(\theta(t)) \\ y(t) = R(t) * \cos(\theta(t)) \end{cases} \begin{cases} R(t) = R_0 * \left(r - \frac{t}{T_{max}}\right) * rand \\ \theta(t) = A * \left(1 - \frac{t}{T_{max}}\right) * rand \end{cases} \begin{cases} x(t) = \frac{x(t)}{max|x(t)|} \\ y(t) = \frac{y(t)}{max|y(t)|} \end{cases} \tag{14}$$

Whereas R_0 characterizes the primary value of radius [0.5, 3], A characterizes the gain of the angle, the value is [5, 15], $rand$ denotes arbitrary gain [0,1], and r denotes gain of the control [1, 2].

Swooping and Stooping Phase

Afterward a low- and a high-flying stage, the RTH concentrates on its prey, at which opinion it is required to search. In this stage, the RTH will jump at the prey to safeguard killer shots; therefore, this behavior is demonstrated utilizing Eq. (15).

$$X(t) = \alpha(t) * X_{best} + x(t) * StepSize1(t) + y(t) * StepSize2(t) \tag{15}$$

DOI: https://doi.org/10.54216/FPA.180202
Received: July 29, 2024 Revised: October 30, 2024 Accepted: January 03, 2025

Whereas $StepSize1(t)$and$StepSize2(t)$is estimated depending on Eq. (16) and Eq. (17).

$$StepSize1(t) = X(t) - TF(t) * X_{mean} \tag{16}$$

$$StepSize2(t) = G(t) * X(t) - TP(t) * X_{best} \tag{17}$$

Whereas α and G characterize the acceleration and gravity factors, correspondingly, and they are established utilizing Eqs. (18) and (19).

$$\alpha(t) = sin^2\left(2.5 - \frac{t}{T_{\max}}\right) \tag{18}$$

$$G(t) = 2 * \left(1 - \frac{t}{T_{\max}}\right) \tag{19}$$

Whereas α epitomizes the acceleration of the hawks, which produces with improving t to increase speed of convergence, whereas G indicates the effect of gravitation, which declines as the hawk approaches the prey thus decreasing exploitation diversities. The RTH's pseudocode is delineated in Algorithm 1.

Algorithm 1: The pseudo-code of the RTH

Start
Initialization: the related parameters.
Initialization: random generation inside the searching region.
While $t < \tau_{\max}$ do
High-soaring phase:
Upgrade the population by Eq. (8)
Low-soaring phase:
Upgrade the population by Eq. (12)
Stooping and Swooping phase:
Upgrade the population by Eq. (15)
$t = t + 1$
End while
return optimal solution
end

The fitness selection is one of the large features that influences the performance of RTH model. The hyperparameter range technique consists of the solution-encrypted system for assessing the effectiveness of the candidate solution. The RTH model reflects precision as the main norm to project the fitness function. Its mathematical formulation is formulated below:

$$Fitness = \max(P) \tag{20}$$

$$P = \frac{TP}{TP + FP} \tag{21}$$

Here, TP signifies the positive value of true and FP denotes the positive value of false.

4. Experimental Validation

This article studies the performance of the BFRPM-AMRTH technique on the German Credit Risk database from Kaggle [20]. The dataset consists of 1000 samples with dual class labels are presented in Table 1.

Table 1: Dataset details

Classes	No. of Instances
Financial Risk	300
Non-Financial Risk	700
Total Instances	1000

Fig. 3 established the classifier outcomes of the BFRPM-AMRTH algorithm on the test dataset. Figs. 3a-3b demonstrates the confusion matrix with correct recognition and classification of every 2 classes on a 70%:30% TRASE/TESSE. Fig. 3c exhibits the PR analysis, signifying superior outcomes over every class. Simultaneously,

DOI: https://doi.org/10.54216/FPA.180202
Received: July 29, 2024 Revised: October 30, 2024 Accepted: January 03, 2025

Fig. 3d illustrates the ROC values, establishing capable outcomes with better ROC analysis for different class labels.

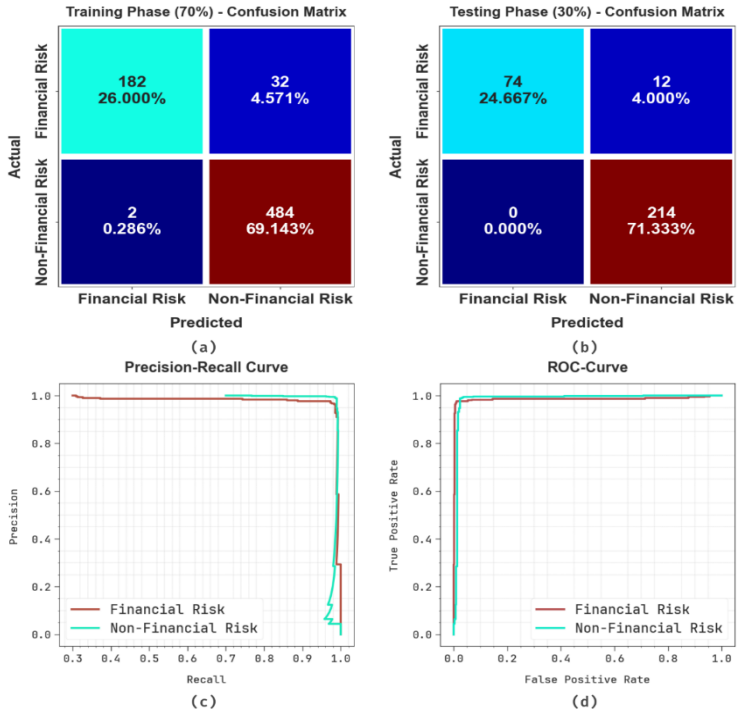

Figure 3. (a-b) Confusion matrix and (c-d) PR and ROC Graphs

In Table 2 and Fig. 4, overall classification results of the BFRPM-AMRTH technique are portrayed for 70%:30% TRASE/TESSE. The tabulated values inferred that the BFRPM-AMRTH technique proficiently recognizes the two classes. On 70%TRASE, the BFRPM-AMRTH approach offers average $accu_y$ of 95.14%, $sens_y$ of 92.32%, $spec_y$ of 92.32%, F_{score} of 94.03%, and MCC of 88.58%. In addition, on 30%TESSE, the BFRPM-AMRTH methodology provides average $accu_y$ of 96.00%, $sens_y$ of 93.02%, $spec_y$ of 93.02%, F_{score} of 94.89%, and MCC of 90.26%.

Table 2: Classifier result of BFRPM-AMRTH approach with 70%:30% TRASE/TESSE

Class Labels	$Accu_y$	$Sens_y$	$Spec_y$	F_{Score}	MCC
Training Phase (70%)					
Financial Risk	95.14	85.05	99.59	91.46	88.58
Non-Financial Risk	95.14	99.59	85.05	96.61	88.58
Average	95.14	92.32	92.32	94.03	88.58
Testing Phase (30%)					
Financial Risk	96.00	86.05	100.00	92.50	90.26
Non-Financial Risk	96.00	100.00	86.05	97.27	90.26
Average	96.00	93.02	93.02	94.89	90.26

DOI: https://doi.org/10.54216/FPA.180202
Received: July 29, 2024 Revised: October 30, 2024 Accepted: January 03, 2025

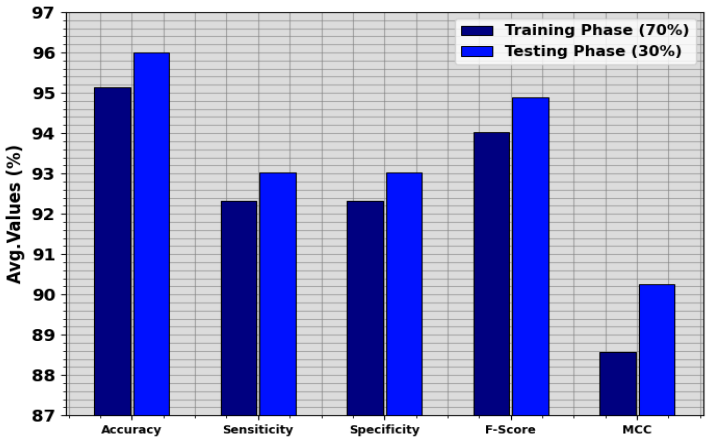

Figure 4. Average result of BFRPM-AMRTH methodology with 70%:30% TRASE/TESSE

In Fig. 5, the TRA $accu_y$ (TRAAY) and validation $accu_y$ (VLAAY) outcomes of the BFRPM-AMRTH technique are illustrated. The $accu_y$analysis are calculated within the range of 0-30 epochs. The figure highlights that the TRAAY and VLAAY values exhibit rising tendencies, which reported the capacity of the BFRPM-AMRTH algorithm with maximum performance across multiple iterations. In addition, the TRAAY and VLAAY leftovers closer across the epochs, which identifies inferior overfitting and demonstrates superior outcomes of the BFRPM-AMRTH approach, assuring continuous prediction on hidden samples.

Figure 5. $Accu_y$ Curve of the BFRPM-AMRTH approach

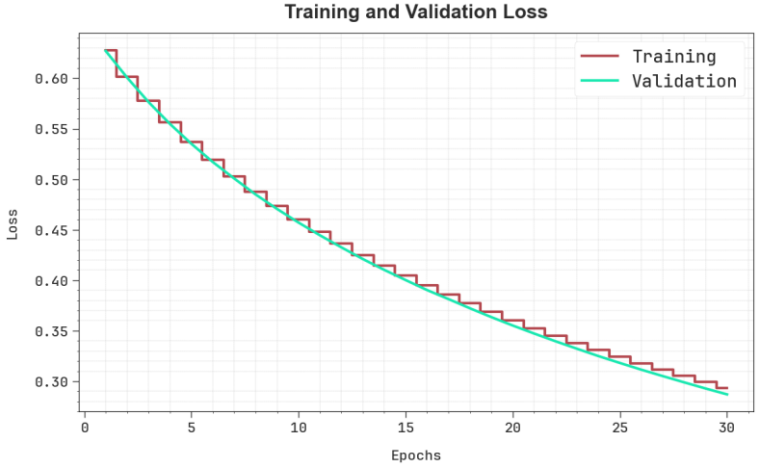

Figure 6. Loss analysis of the BFRPM-AMRTH approach

DOI: https://doi.org/10.54216/FPA.180202
Received: July 29, 2024 Revised: October 30, 2024 Accepted: January 03, 2025

In Fig. 6, the TRA loss (TRALO) and VLA loss (VLALO) curves of the BFRPM-AMRTH technique are shown. The values of loss are computed across an interval of 0-30 epochs. It is presented that the TRALO and VLALO analysis establishes a diminishing trend, which informed the capacity of the BFRPM-AMRTH system in balancing a exchange between data fitting and simplification. The constant reduction in values of loss furthermore pledges the maximal performance of the BFRPM-AMRTH technique and tunes the prediction results in time.

In Table 3, the overall comparison study of the BFRPM-AMRTH technique is clearly portrayed [21].

Table 3: Comparative outcome of BFRPM-AMRTH algorithm with other methodologies

Classifiers	$Sens_y$	$Spec_y$	$Accu_y$	F_{Score}
BFRPM-AMRTH	93.02	93.02	96.00	94.89
HHPODL-FCP	92.59	92.74	94.92	93.74
QABO-LSTM-RNN	87.24	92.58	91.98	90.13
LSTM-RNN Method	82.21	88.55	84.60	88.75
ACO Technique	78.32	69.30	75.80	85.43
MLP Model	73.88	66.90	70.98	75.13
SVM Classifier	72.70	66.42	71.19	71.79
AdaBoost Method	71.41	61.35	67.53	71.27

Fig. 7 examines the comparative $accu_y$ and F_{score} results of the BFRPM-AMRTH technique. The results portrayed that the BFRPM-AMRTH technique reaches better performance. Based on $accu_y$, the BFRPM-AMRTH technique offers higher $accu_y$ of 96.00% whereas the HHPODL-FCP, QABO-LSTM-RNN, LSTM-RNN, ACO, MLP, SVM, and AdaBoost models accomplish lower $accu_y$ of 94.92%, 91.98%, 84.60%, 75.80%, 70.98%, 71.19%, and 67.53%, correspondingly. Followed by, depending on F_{score}, the BFRPM-AMRTH approach provides better F_{score} of 94.89% where the HHPODL-FCP, QABO-LSTM-RNN, LSTM-RNN, ACO, MLP, SVM, and AdaBoost algorithms accomplish lower F_{score} of 93.74%, 90.13%, 88.75%, 85.43%, 75.13%, 71.79%, and 71.27%, respectively.

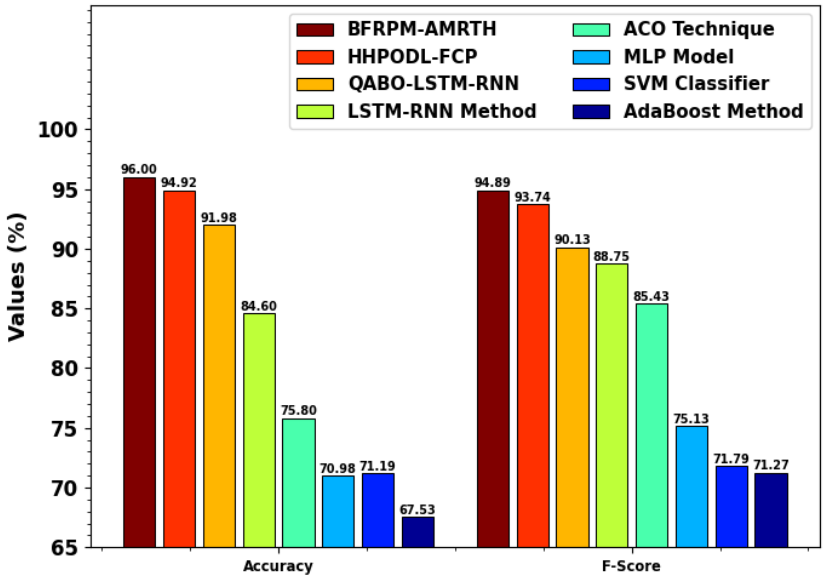

Figure 7. $Accu_y$ and F_{score} outcome of BFRPM-AMRTH algorithm with other models

DOI: https://doi.org/10.54216/FPA.180202
Received: July 29, 2024 Revised: October 30, 2024 Accepted: January 03, 2025

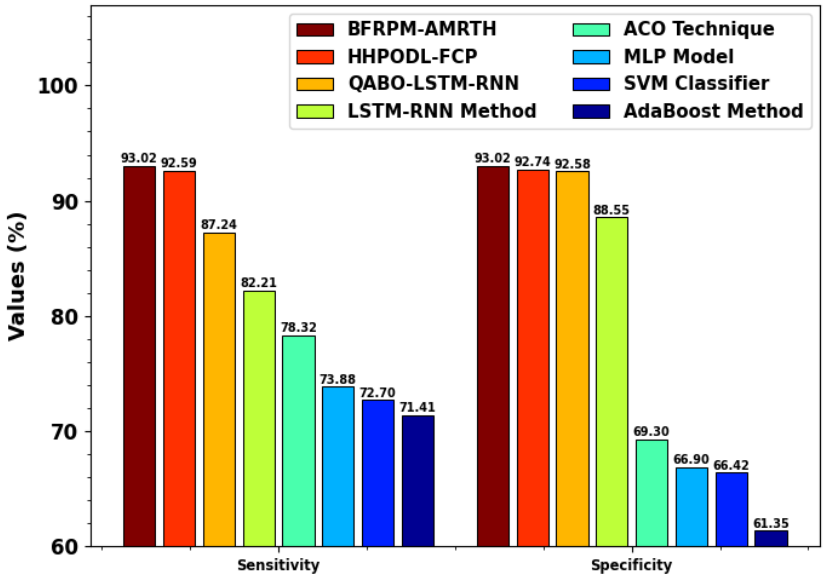

Figure 8. $Sens_y$ and $Spec_y$ outcome of BFRPM-AMRTH algorithm with other models

Fig. 8 inspects the comparative $sens_y$ and $spec_y$ outcomes of the BFRPM-AMRTH system. The outcomes portrayed that the BFRPM-AMRTH algorithm achieves higher performance. Based on $sens_y$, the BFRPM-AMRTH methodology provides maximal $sens_y$ of 93.02% while the HHPODL-FCP, QABO-LSTM-RNN, LSTM-RNN, ACO, MLP, SVM, and AdaBoost approaches reach lesser $sens_y$ of 92.59%, 87.24%, 82.21%, 78.32%, 73.88%, 72.70%, and 71.41%, respectively. Followed by, depend on $spec_y$, the BFRPM-AMRTH system provides greater $spec_y$ of 93.02% where the HHPODL-FCP, QABO-LSTM-RNN, LSTM-RNN, ACO, MLP, SVM, and AdaBoost techniques achieve minimum $spec_y$ of 92.74%, 92.58%, 88.55%, 69.30%, 66.90%, 66.42%, and 61.35%, correspondingly.

5. Conclusion

In this paper, we offer BFRPM-AMRTH Algorithm. The presented BFRPM-AMRTH model aims to address the challenges of identifying and mitigating potential financial threats in a dynamic environment. Initially, the BFRPM-AMRTH technique applies the LSN data normalization technique to standardize the input features and ensure consistency across the dataset. In addition, the LSTMA-AE technique can be employed for classifying financial risks. Eventually, the RTH algorithm adjusts the hyperparameter values of the LSTMA-AE algorithm optimally and outcomes in greater classification performance. To ensure the improved performance of BFRPM-AMRTH system, a huge range of simulation studies has been achieved and the obtained outcomes establish the advancement of the BFRPM-AMRTH system over the existing techniques.

Funding: "This research received no external funding"

Conflicts of Interest: "The authors declare no conflict of interest."

References

[1] K. Keasey and R. Watson, "Financial distress prediction models: a review of their usefulness 1," *Risk Management*, pp. 35–48, 2019.

[2] J. Elliott, B. Bodinier, T. A. Bond, M. Chadeau-Hyam, E. Evangelou, K. G. Moons, A. Dehghan, D. C. Muller, P. Elliott, and I. Tzoulaki, "Predictive accuracy of a polygenic risk score–enhanced prediction model vs a clinical risk score for coronary artery disease," *JAMA*, vol. 323, no. 7, pp. 636–645, 2020.

[3] M. A. Faheem, "AI-driven risk assessment models: Revolutionizing credit scoring and default prediction," *Iconic Research and Engineering Journals*, vol. 5, no. 3, pp. 177–186, 2021.

[4] K. G. Moons, R. F. Wolff, R. D. Riley, P. F. Whiting, M. Westwood, G. S. Collins, J. B. Reitsma, J. Kleijnen, and S. Mallett, "PROBAST: A tool to assess risk of bias and applicability of prediction model studies: Explanation and elaboration," *Annals of Internal Medicine*, vol. 170, no. 1, pp. W1–W33, 2019.

DOI: https://doi.org/10.54216/FPA.180202
Received: July 29, 2024 Revised: October 30, 2024 Accepted: January 03, 2025

[5] N. Mselmi, A. Lahiani, and T. Hamza, "Financial distress prediction: The case of French small and medium-sized firms," *International Review of Financial Analysis*, vol. 50, pp. 67–80, 2017.

[6] H. Zhou, G. Sun, S. Fu, J. Liu, X. Zhou, and J. Zhou, "A big data mining approach of PSO-based BP neural network for financial risk management with IoT," *IEEE Access*, vol. 7, pp. 154035–154043, 2019.

[7] E. I. Altman, M. Iwanicz-Drozdowska, E. K. Laitinen, and A. Suvas, "Financial distress prediction in an international context: A review and empirical analysis of Altman's Z-score model," *Journal of International Financial Management & Accounting*, vol. 28, no. 2, pp. 131–171, 2017.

[8] Y. C. Chang, K. H. Chang, and G. J. Wu, "Application of extreme gradient boosting trees in the construction of credit risk assessment models for financial institutions," *Applied Soft Computing*, vol. 73, pp. 914–920, 2018.

[9] A. N. Seow, Y. O. Choong, K. Moorthy, and L. M. Chan, "Intention to visit Malaysia for medical tourism using the antecedents of theory of planned behaviour: A predictive model," *International Journal of Tourism Research*, vol. 19, no. 3, pp. 383–393, 2017.

[10] M. Saracevic, N. Wang, E. E. Zukorlic, and S. Becirovic, "New model of sustainable supply chain finance based on blockchain technology," *Full Length Article*, vol. 3, no. 2, pp. 61–1, 2021.

[11] J. Luo, W. Zhuo, and B. Xu, "A deep neural network-based assistive decision method for financial risk prediction in carbon trading market," *Journal of Circuits, Systems & Computers*, vol. 33, no. 8, 2024.

[12] Y. Venkateswarlu et al., "An efficient outlier detection with deep learning-based financial crisis prediction model in big data environment," *Computational Intelligence and Neuroscience*, vol. 2022, no. 1, p. 4948947, 2022.

[13] D. Wu, X. Ma, and D. L. Olson, "Financial distress prediction using integrated Z-score and multilayer perceptron neural networks," *Decision Support Systems*, vol. 159, p. 113814, 2022.

[14] C. Ju and Y. Zhu, "Reinforcement learning-based model for enterprise financial asset risk assessment and intelligent decision-making," *Applied and Computational Engineering*, vol. 97, pp. 181–186, 2024.

[15] X. Li, J. Wang, and C. Yang, "Risk prediction in financial management of listed companies based on optimized BP neural network under digital economy," *Neural Computing and Applications*, vol. 35, no. 3, pp. 2045–2058, 2023.

[16] T. Yang, A. Li, J. Xu, G. Su, and J. Wang, "Deep learning model-driven financial risk prediction and analysis," *Applied and Computational Engineering*, vol. 77, pp. 196–202, 2024.

[17] X. Chen and Z. Long, "E-commerce enterprises financial risk prediction based on FA-PSO-LSTM neural network deep learning model," *Sustainability*, vol. 15, no. 7, p. 5882, 2023.

[18] M. Wang et al., "Anomaly detection in multidimensional time series for water injection pump operations based on LSTMA-AE and mechanism constraints," *Scientific Reports*, vol. 15, no. 1, p. 2020, 2025.

[19] M. Wang et al., "Multi-strategy improved red-tailed hawk algorithm for real-environment unmanned aerial vehicle path planning," *Biomimetics*, vol. 10, no. 1, p. 31, 2025.

[20] "German Credit Data," *Kaggle*. [Online]. Available: https://www.kaggle.com/datasets/uciml/german-credit.

[21] I. Katib et al., "Hybrid hunter–prey optimization with deep learning-based fintech for predicting financial crises in the economy and society," *Electronics*, vol. 12, no. 16, p. 3429, 2023.

DOI: https://doi.org/10.54216/FPA.180202
Received: July 29, 2024 Revised: October 30, 2024 Accepted: January 03, 2025